Journal of Chromatography, 186 (1979) 99–116

CHROM. 12,125

ANALYSIS OF KINETICS AND CONCENTRATION DEPENDENCE OF ELECTRON-CAPTURE DETECTOR

W. E. WENTWORTH and E. C. M. CHEN
University of Houston, Chemistry Department, Houston, Texas 77004 (U.S.A.)

SUMMARY

The kinetic model for electron capture has been solved rigorously by numerical integration so that changes in positive ion concentration can be taken into account. In this initial study, rate constants and mode of positive ion removal simulates electron capture using a tritium source in a parallel plate configuration. The numerical analysis can be applied to other geometries and sources of electrons. The results show a different concentration dependence which results from the change in positive ion concentration. The response is a function of the kinetic mechanism.

INTRODUCTION

The electron-capture detector has been demonstrated to be one of the most sensitive and hence valuable selective detectors for gas chromatography. It is especially useful for qualitative or semi-quantitative trace analysis. From a quantitative standpoint, however, one of its limitations is the non-linearity of its response. The determination of the proper function to give a linear relationship with concentration has been the subject of several papers. Lovelock[1] originally suggested that the response is logarithmic by analogy to light absorption. However, later it was shown that the reaction occurs primarily in the field-free period when the detector is operated in the pulse-sampling mode so that the analogy is not very appropriate. A kinetic model for the electron-capture processes for thermal reactions was developed by Wentworth *et al.*[2] which led to the relationship

$$\frac{b - e^-}{e^-} = Ka \tag{1}$$

where b is the electron concentration in the absence of a capturing species, e^- is the electron concentration in the presence of the capturing species, K is the electron capture coefficient, and a is the concentration of the capturing species. This relationship had been proposed earlier by Wentworth and Becker[3] for the case where equilibrium existed. However, eqn. 1 has been shown to be valid for all four of the thermal electron attachment mechanisms which have been reviewed by Wentworth

and Steelhammer[4]. An analog computer for linearizing the electron-capture detector response using this function has been described[5].

Since the time of this work on the analysis of the electron-capture detector, a considerable amount of experimental results in this and related fields have been published. In particular, work in atmospheric pressure ionization mass spectrometry gives direct information on negative and positive ion formation under conditions related to those in the electron-capture detector. With these more recent data it seems appropriate to re-examine the basic kinetic model and the ensuing mathematical analysis. In particular we will focus attention on the concentration dependence which is of greatest concern to analytical chemistry. Analysis of the kinetic model has been carried out by numerical solution of the differential equations, alleviating some of the assumptions that were necessary in the previous mathematical analysis.

Maggs *et al.*[6] have described an alternative method of linearization of the response in the electron-capture detector based upon modulating the frequency of pulsing so that the current is maintained constant. In this case,

$$\frac{f - f_0}{f_0} = Ka \tag{2}$$

where f_0 is the frequency giving the base current in the absence of a capturing species and f is the frequency giving the base current in the presence of the capturing species. This equation was justified for a restricted form of the kinetic model. This technique is easier to automate and is used in several commercial detectors, but there have been reports of non-linearity and non-reproducibility[6]. Several of the instrumental design parameters which can be used to eliminate these problems have been presented by Patterson *et al.*[7]. However, there has been no detailed consideration of the frequency-modulated mode of operation with respect to the general kinetic model of the electron-capture processes. For analytical purposes it is important to know if eqn. 2 for the pulsed frequency mode is expected to hold for all electron attachment processes.

The numerical analysis described in this paper can be used to evaluate the pulsed frequency mode expected from this kinetic model. This will be done in a subsequent paper when we carry out a similar analysis for the nickel-63 electron-capture detector.

As we will see shortly, it appears that the kinetic analysis depends significantly on the mode at which positive ions are removed from the reaction zone. This in turn must depend on the geometry of the cell, the field strength of the pulsed potential, and the nature of the radioactive foil. For example, the original electron-capture detector cells used tritium foils in a parallel plate configuration, making the field strength somewhat uniform. Because of the short range of tritium β-particles, the reaction zone is confined within *ca.* 2 mm of the foil and *ca.* 8 mm away from the sampling electrode[2]. On the other hand, nickel-63 foils cannot be used in a similar parallel plate configuration apparently because the range of β-particles is too great. Spurious results occur if the β-rays are allowed to strike the collecting electrode. Alternatively, the nickel-63 foil is placed on the walls of a cylinder and the collecting electrode consists of a very small diameter rod or wire along the axis of the cylinder. The nickel-63 β-rays produce ionization throughout the cell, even in the vicinity of the collecting electrode. Consequently, it is not surprising that positive ions can migrate to the

collecting electrode during field free conditions[8]. The applied field when the foil is pulsed negatively is non-uniform from the central wire to the cylinder wall. The situation is even more complicated when the central wire or rod protrudes only up to the cylinder (pin-in-cup design), giving an extremely inhomogeneous field when a potential is applied. Consequently, it is obvious that the mode at which positive ions can be removed from a detector can depend on the cell geometry and allied field. For this reason we have restricted our initial analysis essentially to the simpler parallel plate, tritium foil electron-capture detector. In later studies we will consider other electron-capture detector geometries, applied fields, and the use of the more versatile nickel-63 foil, which can be operated at a higher temperature.

KINETIC MODEL

The kinetic model for electron capture has been presented in earlier publications[3,4]. In general, this model has been well received and the majority of data obtained since the development of the model supports its general validity. However, there is one major misconception concerning the model which has been propagated in various review articles on electron-capture mechanisms[9–11]. This involves the relative magnitude of the rate constant for recombination of negative ions with positive ions compared to the magnitude of the rate constant for recombination of electrons with positive ions. The review articles state that the negative ion recombination coefficient is five to eight orders of magnitude greater than the electron recombination, whereas the original article[2] presents data showing that the two rate constants are about the same order of magnitude with the negative ion recombination rate constant being at most a factor of eight greater than the electron recombination rate constant.

For convenience to the reader, the kinetic model is summarized in the following reaction sequence, where AB represents any polyatomic molecule capable of capturing or attaching an electron:

$$\beta + (\mathrm{Ar} + 10\%\ \mathrm{CH_4}) \xrightarrow{k_p R_\beta} \mathrm{e^-} + \oplus + R + \beta^* \tag{3}$$

$$\mathrm{e^-} + \oplus \xrightarrow{k'_D} \text{neutral species} \tag{4}$$

$$\mathrm{e^-} + \mathrm{AB} \xrightarrow{k_{12}} \mathrm{A} + \mathrm{B^-} \tag{5}$$

$$\mathrm{e^-} + \mathrm{AB} \xrightarrow{k_1} \mathrm{AB^-} \tag{6}$$

$$\mathrm{AB^-} \xrightarrow{k_{-1}} \mathrm{AB} + \mathrm{e^-} \tag{7}$$

$$\mathrm{AB^-} \xrightarrow{k_2} \mathrm{A} + \mathrm{B^-} \tag{8}$$

$$\mathrm{AB^-} + \oplus \xrightarrow{k'_{N1}} \text{neutral species} \tag{9}$$

$$\mathrm{B^-} + \oplus \xrightarrow{k'_{N2}} \text{neutral species} \tag{10}$$

where β^* designates the β-particle with reduced energy as a result of the ion pair formation. Generally β^* contains sufficient energy to cause subsequent formation of ion pairs. Each ion pair formation requires *ca.* 40 eV and a single β-particle with energy in the keV or MeV range can form numerous ion pairs in the carrier gas. The rate constant $k_p R_\beta$ is used to represent the overall rate of ion pair formation.

In this kinetic scheme several reaction steps may involve collision with a neutral species to either add or remove the necessary energy for the reaction to take place. This would increase the order of the reaction step. However, at high pressures (*ca.* 1 atm) these neutral species will be at comparatively high concentration compared to the capturing species AB or the ionic species and will remain constant. For this reason they are not shown explicitly in the kinetic mechanism.

If the electron attachment process forms AB^- which does not dissociate according to reaction 7, then it is impossible to differentiate kinetically between reactions 5 and 6 in terms of electron capture. For this reason in the subsequent rate expressions we have left out reaction 5, and Mechanism β, as we define it later, will inherently describe also electron attachment via reaction 5. Generally reactions 5 and 6 differ in that reaction 5 frequently can have a significant activation energy whereas for reaction 6 the activation energy is generally small.

The rate expressions describing the change in concentration of the various species between pulses for reactions 3, 4 and 6–10 are given by:

$$\frac{d[b]}{dt} = \frac{d[\oplus_0]}{dt} = k_p R_\beta - k'_D[\oplus_0]\,[b] \tag{11}$$

$$\frac{d[e^-]}{dt} = k_p R_\beta - k'_D[\oplus]\,[e^-] - k_1[AB]\,[e^-] + k_{-1}[AB^-] \tag{12}$$

$$\frac{d[\oplus]}{dt} = k_p R_\beta - k'_D[\oplus]\,[e^-] - k'_{N1}[\oplus]\,[AB^-] - k'_{N2}[\oplus]\,[B^-] \tag{13}$$

$$\frac{d[AB^-]}{dt} = k_1[AB]\,[e^-] - k_{-1}[AB^-] - k'_{N1}[\oplus]\,[AB^-] - k_2[AB^-] \tag{14}$$

$$\frac{d[B^-]}{dt} = k_2[AB^-] - k'_{N2}[\oplus]\,[B^-] \tag{15}$$

where $[b]$ = concentration of electrons when no capturing species is present, $[\oplus_0]$ = concentration of positive species in the absence of capturing species, and the remaining ion concentrations $[e^-]$, $[\oplus]$, $[AB^-]$, $[B^-]$ are those when the capturing species AB is present.

NUMERICAL SOLUTION

In the previous analysis of this kinetic model[2] the positive ion concentration was assumed to build up to a constant value as a result of electron withdrawal by the applied negative pulsed potential. Furthermore, it was assumed that the positive ion

concentration did not change significantly when the electron-capturing species is present. This simplified the mathematical analysis since the differential equations could be solved explicitly for the electron concentration. The effect of the pulsed potential was inherently accounted for in the build up of the positive ion concentration.

However, in a recent study[8] it was shown that the positive ion concentration decreases at the same time that the electron concentration decreases. For this reason a rigorous solution of the differential equations must consider the positive ion concentration as a variable. In addition the mode of removing the positive ions must be specified and the solution of the differential equations repeated through numerous pulsed cycles until a steady state is reached. This procedure must be carried out for each specified pulse period, t_p, and concentration. For a complete set of concentrations at various pulse periods these calculations can be time consuming. This is especially true for the higher concentrations where the differential equations show greater changes in rates and the numerical solution requires smaller time increments in the integration.

The differential eqns. 11–15 were integrated numerically assuming the concentration of AB remains constant, which is a reasonably good assumption under normal electron-capture operation. The procedure for the numerical integration is described in the Appendix at the end of the paper. At the completion of the integration over the time of the designated pulse period, t_p, the electrons were removed as anticipated by the application of a negative potential commonly practiced in pulsed electron-capture operation. For the calculations in this paper a small fraction (f) of the positive ion concentration was also removed at this time. This mode of positive ion removal simulates the collection of a fraction of the positive ions at the cathode where the pulsed negative potential is applied. This mode of positive ion removal would apply most likely to the parallel plate tritium electron-capture detector where the positive ions are in close proximity to the cathode. Other processes for positive ion removal could also be important, especially at long pulse intervals. These will be considered in subsequent studies. For this initial work we have restricted the positive ion removal to a single process. Most certainly for the nickel-63 detector other modes of positive ion loss must be considered since the positive ions are distributed throughout the cell, far removed from the cathode.

This process was repeated as in the operation of an electron-capture detector until a steady state of electron concentration at the duration of the pulse period was attained. The criterion for steady state was a change in electron concentration of less than one part in 10,000. In practice, extrapolation techniques were used so that steady state could be reached more rapidly, thus decreasing the computational time. The procedure for extrapolation is described in the Appendix.

KINETIC MECHANISMS

In an earlier review paper[4] the electron attachment mechanisms were classified into four mechanisms based on the nature of the potential energy curves of the negative ion in relationship to that of the neutral species. In a later paper[12] three *kinetic* mechanisms were defined in terms of the relative magnitude of the rate constants and identification with the previously defined four mechanisms was made. We

will follow this same classification in this paper where we have replaced k_L with k'_{N1} [⊕]

β: k'_{N1} [⊕] $> k_{-1} > k_2$ Mechanisms I, III, IV at low T and Mechanism II

α: $k_{-1} > k'_{N1}$ [⊕] $> k_2$ Mechanism I at high T
Mechanism III, IV at intermediate T

γ: $k_{-1} > k_2 > k'_{N1}$ [⊕] Mechanism III, IV at high T

The expressions for the capture coefficients at steady state K_∞ have been expressed in terms k'_D and k'_N since we are now assuming that the positive ion concentration can change. In principle a fourth kinetic mechanism could occur where $k_2 > k_{-1} > k'_{N1}$ [⊕] and this would give K_∞ identical to Mechanism β. However, there have been no published data supporting this fourth mechanism so we will not consider it at this time.

ELECTRON CONCENTRATION DEPENDENCE ON PULSE PERIOD

The electron concentration in the electron-capture detector when no capturing species is present is found by solving the differential equations given in eqn. 11. The initial slope of the electron concentration *versus* pulse period is given by $k_p R_\beta$ which in turn is dependent on the activity of the radioactive source. The value of $k_p R_\beta$ does not affect the slopes of the electron concentration *versus* t_p curve, but only the overall magnitude. In our calculations we selected a value of $4 \cdot 10^{-10}$ mole/l sec which is typical of a tritium source of 150 mCi.

In our initial solution of eqn. 11 we examined the electron concentration as a function of pulse period for different k_D and f values. It was noted that the ratio of electron to positive ion concentration remained constant for any curve and in fact the ratio was simply the fraction (f) of positive ions removed at the end of the pulse period

$$f = \frac{b}{[\oplus_0]} \tag{16}$$

This is understandable since the removal of electrons by pulsing at the end of any pulse period must equal the removal of positive ions other than by recombination. Since $[\oplus_0]$ is given by b/f in eqn. 11, the steady state expression at $t_p = \infty$ is given by

$$\frac{db}{dt} = 0 = k_p R_\beta - \frac{k'_D}{f}(b^\infty)^2$$

The initial slope at $t_p = 0$ ($b = 0$) is

$$\left(\frac{db}{dt}\right)_{t_p=0} = k_p R_\beta$$

The constant $k_p R_\beta$ can be evaluated from the initial slope and k_D/f from

$$\frac{k'_D}{f} = \frac{\text{initial slope}}{(b^\infty)^2}$$

In order to illustrate the agreement between the numerical solution to eqn. 11 and experiment, we show in Fig. 1 the experimental graph of Van de Wiel and Tommassen[13] for ionization of argon + 10% methane. The calculated curve agrees well with the experimental curve except in the region of 3000 μsec. The experimental curve tends to plateau sooner than the calculated curve and this can only occur by removal of more positive ions at shorter pulse intervals, allowing the electron concentration to increase. Our calculations remove more positive ions at shorter intervals compared to removal by other mechanisms, such as diffusion. Consequently, we cannot account for the discrepancy in the two curves. If one assumes the positive ion concentration remains constant, independent of pulse intervals, this results in an even greater discrepancy with the experimental curve.

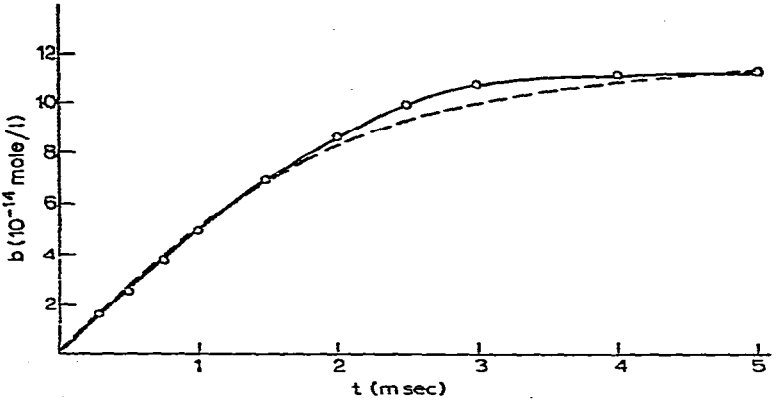

Fig. 1. Electron concentration *versus* pulse period. ———, Experimental curve; – – –, calculated curve.

It should be noted, in Fig. 1, that no maximum occurs in the calculated curve, regardless of the choice of constants. This is in agreement with Van de Wiel and Tommassen[13], who have shown that the maximum in this type of graph arises from contamination of the detector with oxygen.

CONCENTRATION DEPENDENCE AT STEADY STATE

In order to arrive at the concentration dependence predicted by the kinetic model the differential rate expressions in eqns. 11–15 were solved numerically over the pulse period and this was repeated until a constant concentration of ionic species was observed. The calculations were made for different concentrations of capturing species and pulse intervals for the three mechanisms described previously. However, before discussing these results we will first derive the expected concentration dependence at long pulse intervals and we can then examine the data to see how well these relationships hold at shorter pulse intervals.

Assuming steady state for b, e^-, and AB^- we set eqns. 11, 12 and 14 to zero.

$$0 = k_\beta R_\beta - k'_D[\oplus_0]b \tag{18}$$

$$0 = k_\beta R_\beta - k'_D[\oplus]\,[e^-] - k_1[AB]\,[e^-] + k_{-1}[AB^-] \tag{19}$$

$$0 = k_1\,[AB]\,[e^-] - k_{-1}\,[AB^-] - k'_{N1}\,[\oplus]\,[AB^-] - k_2\,[AB] \tag{20}$$

Solving eqn. 20 for $[AB^-]$ and eqn. 18 for $k_\beta R_\beta$, substitution into eqn. 19 reduces to

$$\frac{b}{[e^-]} = \frac{[\oplus]}{[\oplus_0]} + \frac{k_1(k_2 + k'_{N1}[\oplus])}{k'_D[\oplus_0]\,[k_{-1} + k_2 + k'_{N1}\oplus]}\,[AB] \tag{21}$$

Obviously if $[\oplus] = [\oplus_0]$ then the expression reduces to that derived previously[12]. However, it has been our observation from the numerical solutions that regardless of the concentration of AB, pulse period, or mechanism, at steady state the ratio of concentration of electrons to positive ions at steady state remains approximately constant, equal to the fraction (f) of positive ions removed at the end of each pulse period.

$$\frac{[e^-]}{[\oplus]} = f \tag{22}$$

As with eqn. 16, this result can be rationalized on the basis of removal of equal amounts of electrons and positive ions, thus requiring a higher concentration of positive ions to offset the fact that only a fraction (f) is removed. In any event, eqns. 16 and 22 can be justified on an empirical basis and substitution into eqn. 21 reduces to

$$\frac{b^2 - [e^-]^2}{b[e^-]} = \frac{k_1(k_2 + k'_{N1}[\oplus])}{k'_D[\oplus_0]\,(k_{-1} + k_2 + k'_{N1}[\oplus]}\,[AB] \tag{23}$$

This equation can be reduced to simpler expressions for each of the mechanisms.

Mechanism β: $k'_{N_1}[\oplus] > k_{-1} > k_2$

$$\frac{b^2 - [e^-]^2}{b[e^-]} = \frac{k_1}{k'_D[\oplus_0]}\,[AB] \tag{24}$$

Since $[\oplus_0]$ will remain constant we expect

$$\frac{b^2 - [e^-]^2}{b[e^-]} = K_\infty[AB] \tag{25}$$

where

$$K_\infty = \frac{k_1}{k'_D[\oplus_0]} = \frac{k_1 f}{k'_D b} \tag{26}$$

Mechanism α: $k_{-1} > k'_{N1}[\oplus] > k_2$

$$\frac{b^2 - [e^-]^2}{b[e^-]} = \frac{k_1 k'_{N1}[\oplus]}{k'_D[\oplus_0]k_{-1}}[AB] \tag{27}$$

Substitution of $[\oplus]$ and $[\oplus_0]$ with eqns. 16 and 22 gives

$$\frac{b^2 - [e^-]^2}{[e^-]^2} = K_\infty[AB] \tag{28}$$

where

$$K_\infty = \frac{k_1 k'_{N_1}}{k_{-1}k'_D} \tag{29}$$

Mechanism γ: $k_{-1} > k_2 > k'_{N1}[\oplus]$

$$\frac{b^2 - [e^-]^2}{b[e^-]} = \frac{k_1 k_2}{k'_D[\oplus_0]k_{-1}}[AB] \tag{30}$$

Again $[\oplus_0]$ will remain constant and

$$\frac{b^2 - [e^-]^2}{b[e^-]} = K_\infty[AB] \tag{31}$$

where

$$K_\infty = \frac{k_1 k_2}{k_{-1}k'_D[\oplus_0]} = \frac{k_1 k_2 f}{k_{-1} b} \tag{32}$$

Obviously from eqns. 25 and 31 we expect the function $(b^2 - [e^-]^2)/b[e^-]$ to be linear with concentration at long pulse intervals for Mechanisms β and γ. Mechanism β is probably the most prevalent since it encompasses dissociative as well as non-dissociative attachment. For Mechanism α we expect the function $(b^2 - [e^-]^2)/[e^-]^2$ to be linear with concentration at long pulse intervals.

It is interesting to note that both of these functions reduce to $(b - [e^-])/[e^-]$ at low capture where $[e^-]$ approaches b:

$$\frac{b^2 - [e^-]^2}{b[e^-]} = \frac{b - [e^-]}{[e^-]} \quad \frac{b + [e^-]}{b} \approx \frac{b - [e^-]}{[e^-]} \cdot 2$$

$$\frac{b^2 - [e^-]^2}{[e^-]^2} = \frac{b - [e^-]}{[e^-]} \quad \frac{b + [e^-]}{[e^-]} \approx \frac{b - [e^-]}{[e^-]} \cdot 2$$

The factor of 2 in each case would be incorporated into K.

However, at concentrations where you get a high percent capture the functions in eqns. 25, 28 and 31 will differ considerably from $(b - [e^-])/[e^-]$. At high capture the two functions should show deviations in the opposite directions. For Mechanisms β and γ, as given in eqns. 24 and 30, a graph of $(b - [e^-])/[e^-]$ *versus* concentration should show positive deviations from linearity since $(b + [e^-])/b$ decreases from 2 down to a lower limit of one. However, for Mechanism α, as given in eqn. 27, a graph of $(b - [e^-])/[e^-]$ should show negative deviations from linearity since $(b + [e^-]/[e^-]$ increases from 2 to unlimited values as $[e^-]$ decreases.

RESULT OF NUMERICAL INTEGRATION

Mechanism β

In order to examine numerically the concentration dependence predicted by the kinetic model we have selected the following rate constants which will result in kinetic Mechanism β:

$$k_p R_\beta = 4 \cdot 10^{-10} \text{ mole/l sec}$$

$$k'_D = 2 \cdot 10^{14} \text{ l/mole sec}$$

$$k_1 = 2.7 \cdot 10^{12} \text{ l/mole sec}$$

$$k_{-1} = k_2 = k'_{N_2} = 0$$

$$k'_{N_1} = 1.6 \cdot 10^{15} \text{ l/mole sec}$$

The k_1 rate constant is that for anthracene[2]. An f value of 0.02 gave an appropriate k_D to simulate the current in an argon–methane carrier gas with a tritium foil[2]. Numerical solutions were carried out for AB concentrations in the range $1 \cdot 10^{-8}$ to $1 \cdot 10^{-6}$ mole/l and pulse intervals from 100 to 2000 μsec.

As we have just shown, at long pulse intervals the function $(b^2 - [e^-]^2)/b[e^-]$ is expected to be directly proportional to the concentration of capturing species. For this reason we have calculated this function even at shorter pulse intervals to see how well it fits a linear relationship with concentration. The results are given in Fig. 2. The straight lines have been drawn with a slope of one so the deviations give a true representation of the deviation from the linear relationship between $(b^2 - [e^-]^2)/b[e^-]$ and AB. As shown by the graphs in Fig. 2, the calculated data fit the linear function quite well, even at the shorter pulse intervals. The greatest deviations occur at pulse intervals of 500 and 1000 μsec. The largest deviation of 5.1 % occurs at $[AB] = 1 \cdot 10^{-8}$ mole/l at a pulse interval of 500 μsec. As expected, the electron-capture coefficient increases as the pulse interval increases, approaching the upper limit at 4000 μsec. The results shown in Fig. 2 are most significant in view of the fact that Mechanism β is the most common attachment process. Mechanism β encompasses both dissociative electron capture and non-dissociative capture to compounds with high electron affinities (> 1 eV).

In Fig. 3 we have shown the graph of $(b - [e^-])/[e^-]$ *versus* concentration. Again a log–log graph is used and the linear relationship must fit the straight line with slope of unity, as shown by the dashed lines. The expected increase of a factor of

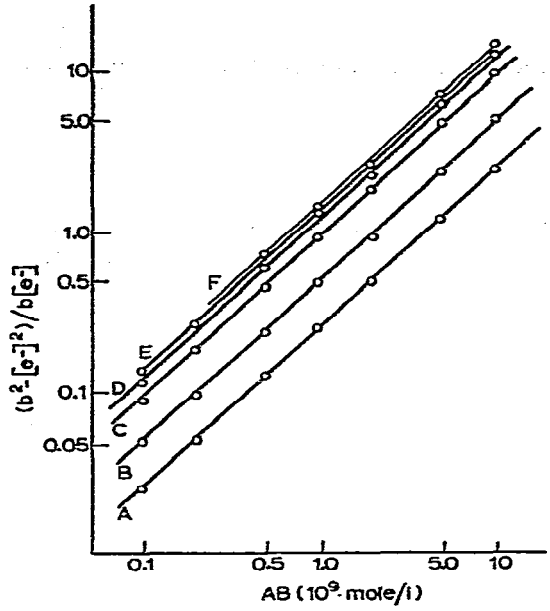

Fig. 2. Calculated concentration dependence for Mechanism β; $(b^2 - [e^-]^2)/b[e^-]$ *versus* concentration at pulse periods: (A) 100 μsec, (B) 200 μsec, (C) 500 μsec. (D) 1000 μsec, (E) 2000 μsec and (F) 4000 μsec.

2 in the capture coefficient as we go to high capture is clearly shown at long pulse intervals. On a log–log graph this factor of 2 is shown by a displacement of log 2 = 0.693 which is very close to that observed at $t_p = 2000$ μsec.

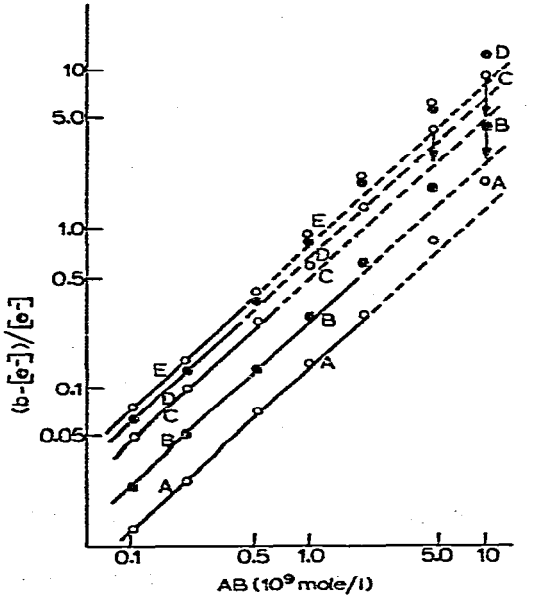

Fig. 3. Calculated concentration dependence for Mechanism β; $(b - [e^-])/[e^-]$ *versus* concentration at pulse periods: (A) 100 μsec, (B) 200 μsec, (C) 500 μsec, (D) 1000 μsec, and (E) 2000 μsec.

Mechanism α

The same rate constants as for Mechanism β were used for the numerical calculations with the exception that

$$k_{-1} = 1.538 \cdot 10^6 \text{ sec}^{-1}$$

which corresponds to anthracene at $T = 573°K$. This temperature is above that permitted for a tritium electron-capture detector but it was chosen so that the criterion for Mechanism α was clearly obeyed

$$k_{-1} \gg k'_{N_1}[\oplus]$$

The highest value for $[\oplus]$ is at long pulse intervals with no capturing species present and at these conditions

$$k'_{N_1}[\oplus] = 1.585 \cdot 10^4 \text{ sec}^{-1}$$

The rate constant k_{-1} is thus *ca.* 100 greater than $k_{N1}[\oplus]$.

The results of the concentration dependence for this mechanism are shown in Fig. 4. For this mechanism we expect $(b^2 - [e^-]^2)/[e^-]^2$ to be linearly related to concentration at long pulse intervals, according to eqn. 28. For this reason this function is graphed in Fig. 4. Again the graph is log–log and the linear function should be represented by a straight line with unit slope. The deviations are different for different pulse intervals. At 100 μsec the positive deviations become very large as the concentration increases. At a concentration of $1 \cdot 10^{-6}$ mole/l the deviation is on the order of 40%. At 200 μsec we see slight positive deviations at low concentration increasing to *ca.* 17% as the concentration is increased to $1 \cdot 10^{-6}$ mole/l. At 500 μsec the deviations are small at low concentrations, but become large positively at higher concentrations (*ca.* 7%). At 1000 μsec only two concentrations were run but the deviation, as expected, becomes much smaller (*ca.* 2–3%) at this long pulse interval. Only one point was calculated at 2000 μsec and the capture coefficient is only a little large than that at 1000 μsec. The behavior for Mechanism α is quite different from that for Mechanism β and at low pulse intervals does not fit the function predicted for long pulse intervals. This is especially significant when one considers that the extent of capture was almost an order of magnitude lower for the calculations for Mechanism α compared to Mechanism β.

The graph of $(b - [e^-])/[e^-]$ *versus* concentration for Mechanism α is shown in Fig. 5. At 100 μsec pulse period the function is surprisingly quite linear. Of course one must realize that the capture is less than 50% even at the highest concentration. At pulse interval 200 μsec the function is linear at low concentrations but begins to show the expected negative deviations at high concentrations. The negative deviations are greater at 500 μsec and should continue to show even more dramatic deviations at higher capture where $b/[e^-]$ becomes very large. The contrast between the negative deviations for Mechanism α and the positive deviations for Mechanism β should be noted.

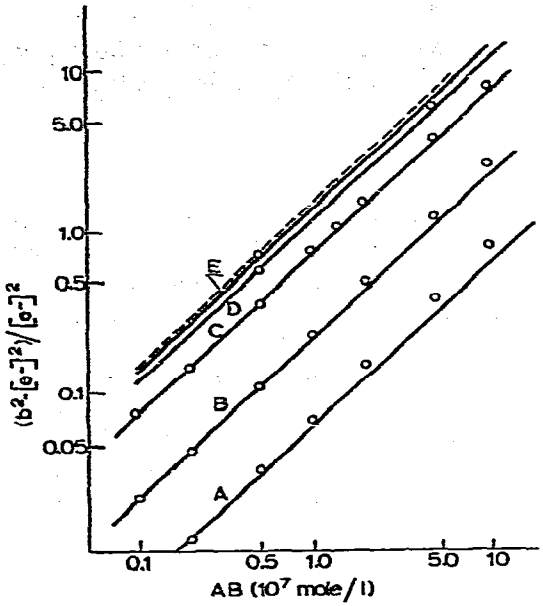

Fig. 4. Calculated concentration dependence for Mechanism α; $(b^2 - [e^-]^2)/[e^-]^2$ *versus* concentration at pulse periods: (A) 100 μsec, (B) 200 μsec, (C) 500 μsec, (D) 1000 μsec, and (E) 2000 μsec.

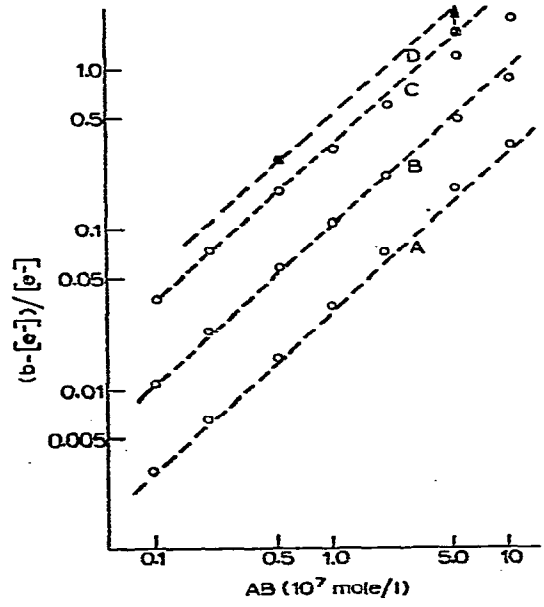

Fig. 5. Calculated concentration dependence for Mechanism α; $(b - [e^-])/[e^-]$ *versus* concentration at pulse periods: (A) 100 μsec, (B) 200 μsec, (C) 500 μsec, and (D) 1000 μsec.

Mechanism γ

In order to simulate data for this mechanism the same rate constants were used as for Mechanism α except for k_2 which was set at $5 \cdot 10^4$ sec^{-1}. This satisfies the criterion for this mechanism

$$k_{-1} > k_2 > k'_{N_1}[\oplus]$$

The numerical solution for this mechanism, as well as Mechanism α, requires rather small time increments and this increases the computational time. For this reason, and the fact that Mechanism γ is not encountered too frequently, the calculations for this mechanism were less extensive. Numerical solutions were made for pulse intervals of 100, 200, and 500 μsec.

According to eqn. 31, we expect the function $(b^2 - [e^-]^2)/b[e^-]$ to be linear with concentration, similar to Mechanism β. A log–log graph of this function is shown in Fig. 6 and an excellent linear relationship is found even at short pulse intervals. The good agreement in Fig. 6 is very similar to that for Mechanism β in Fig. 2. This may not be too surprising since the same functional relationship with concentration at long pulse intervals is expected.

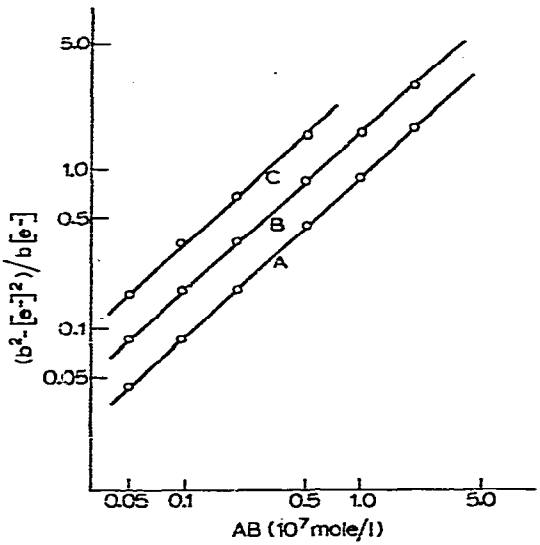

Fig. 6. Calculated concentration dependence for Mechanism γ; $(b^2 - [e^-]^2)/b[e^-]$ *versus* concentration at pulse periods: (A) 100 μsec, (B) 200 μsec, and (C) 500 μsec.

The graph of $(b - [e^-])/[e^-]$ *versus* concentration shows positive deviations almost identical to that for Mechanism β in Fig. 3. It appears from these calculations that we would expect the dependence on concentration to be similar for Mechanisms β and γ.

CORRELATION WITH EXPERIMENTAL RESULTS

As stated earlier, the mode of positive ion removal and the rate constants $k_p R_\beta$ and k'_D used in this initial study are more appropriate to a parallel plate tritium

detector. Therefore, we have taken data from that type detector to correlate with the type of concentration dependence derived from the numerical calculations in this paper. Data of this type are somewhat limited since nickel-63 has been employed more extensively in the past several years.

In order to evaluate the concentration dependence for different mechanisms it is necessary to have electron-capture data over a large concentration range, especially in the region of high capture. Recall that deviations from $(b - [e^-])/[e^-]$ are most pronounced at high capture. Some data of that nature were collected in an earlier study[2] and this will be used for the correlation with the numerical solutions.

Anthracene electron capture follows Mechanism β in the low temperature region (< 163°C). Electron-capture data for anthracene at 101°C are shown in Fig. 7 where both $(b - [e^-])/[e^-]$ and $(b^2 - [e^-]^2)/b[e^-]$ are shown as a function of concentration. Note that at high capture the $(b - [e^-])/[e^-]$ curve shows positive deviation from linearity (dashed line at unit slope). On the other hand, the graph of $(b^2 - [e^-]^2)/b[e^-]$ appears to be reasonably linear although the data do show some deviation at the extremes of high and low capture. In general we have noted that electron capture by compounds which fall into Mechanism β tend to show positive deviations from the $(b - [e^-])/[e^-]$ function at high capture, which is consistent with our numerical calculations in this study.

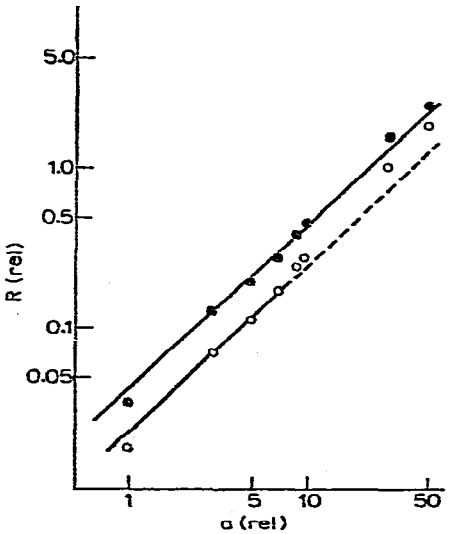

Fig. 7. Experimental values for the corrected response *versus* relative concentration; anthracene at 374 °K. ⊙, $(b - [e^-])/[e^-]$; ⊗, $(b^2 - [e^-]^2)/b[e^-]$.

For compounds which capture electrons according to Mechanism α, we have selected acetophenone and benzanthracene. The temperature dependence of electron capture of acetophenone suggests that Mechanism α occurs at all temperatures in the range 6–200°C[14]. The data as a function of concentration[15] are shown in Fig. 8. The temperature dependence of the electron capture for benzanthracene[2] suggests that capture at high temperature (> 170°C) occurs via Mechanism α. The dependence on

concentration is also shown in Fig. 8. Note that for both compounds the function $(b - [e^-])/[e^-]$ shows negative deviations at high capture, as our numerical calculations revealed. The function $(b^2 - [e^-]^2)/[e^-]^2$ appears to account for these deviations and gives a reasonably good linear relationship.

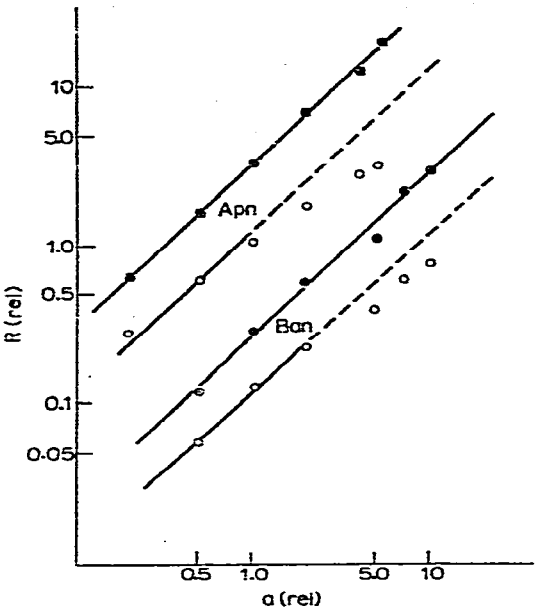

Fig. 8. Experimental values for the corrected response *versus* relative concentration of acetophenone (Apn) at 403 °K and benzanthracene (Ban) at 477 °K. ⊙, $(b - [e^-])/[e^-]$; ⊗, $(b^2 - [e^-]^2)/[e^-]^2$.

CONCLUSIONS

The differential equations arising from the kinetic model for electron capture can be solved rigorously by numerical integration. In particular the positive ion concentration can be taken as a variable and any changes in this quantity can be evaluated. As a result of these calculations we have arrived at the following conclusions from this study:

1. The calculation of the electron concentration at the end of each pulse period has been calculated as a function of pulse period and the curve shows no maximum, which is in agreement with experiment when a clean carrier gas is used.

2. For electron capture by Mechanisms β and γ the calculations reveal that the function $(b - [e^-])/[e^-]$ *versus* concentration should show positive deviations at high capture. The function $(b^2 - [e^-]^2)/b[e^-]$ should give a linear relationship at long pulse intervals, but works rather well even at lower pulse intervals.

3. For electron capture by Mechanism α the calculations show that the function $(b - [e^-])/[e^-]$ *versus* concentration should show negative deviations. These deviations appear to be less significant at lower pulse intervals (100 or 200 μsec) but are significant at long pulse intervals. At long pulse intervals the function $(b^2 - [e^-]^2)/[e^-]^2$ should be linear with concentration. The calculations show that this function gives a satisfactory linear relationship at pulse intervals of 500 μsec and longer.

The model used in these calculations most closely simulates electron capture using a parallel plate electron-capture detector with a tritium source. The mode of positive ion removal is inherent in the model and this will change with cell geometry and the ionizing source. A similar type analysis can be carried out for other electron-capture detectors employing other ionizing sources such as nickel-63.

ACKNOWLEDGEMENTS

Financial support for this work, provided by the Robert A. Welch Foundation, is greatly appreciated.

APPENDIX

The numerical solution to the differential equations was carried out by a simple summation of the derivative times a small time increment. The use of higher order numerical methods was considered but the benefit of possibly using a slightly larger time increment did not seem to be justified. Alternatively, an effort was made to use a variable time increment which not only speeds up the calculations, but also should lead to lower round off errors. The accuracy of the results were checked by changing the time increment and observing what change it made in the final answer. Generally, at least 3 or 4 significant figures were retained in the final electron concentration. Generally, one can see from the graphs in Figs. 2–6 that the data fall on smoothly varying curves or on straight lines and this is indicative of sufficient precision in the calculations. The calculations were started with good first approximation to $[e^-]$, calculated from the expected capture coefficient and the expected value for b from previous calculations.

The numerical integration at the beginning of a cycle requires a smaller increment of time than later in the cycle. This arises from the large derivatives for $d[AB^-]/dt$ and $d[e^-]/dt$ and the rapid change that they undergo during the first part of the cycle. For this reason the time increment was taken to be inversely proportional to these derivatives. The proportionality constants were adjusted so that the integration through the first part of the cycle occurred rapidly but with sufficient accuracy. Generally it was necessary to adjust these proportionality constants for different AB concentrations and the type mechanism. Their use was especially critical for Mechanisms α and γ at high concentrations of AB. The remaining portion of the integration was carried out with a constant time increment varying from 5 μsec down to 0.1 sec.

The numerical integration of the differential equations was carried out over the time of the pulse period. At this time all of the electrons and a small fraction of the positive ions are removed as a result of the applied potential. The integration was then started for the next pulse period and the process is repeated until the concentrations at the end of the pulse period reach a steady state. If this process were carried out literally the calculation time would generally be very long. Fortunately one can recognize a trend in the positive ion concentration and an extrapolation can be made to the final steady state value. However, after an extrapolation was made the integration over successive cycles was repeated until the criterion that $[e^-]$ did not change in one part in 10^5 was met.

The positive ion concentrations at the end of successive integration periods

were examined and it was noted that the differences fit a geometric series quite well; *i.e.* the ratio (r) of successive differences appears to be a constant. The sum of the geometric series can then be calculated

$$S = \frac{\Delta_1}{1 - r}$$

where Δ_1 is the difference in positive ion concentrations. This sum is then added to the positive ion concentration at the beginning of this series to obtain the extrapolated estimate of $[\oplus]$ at steady state. A similar procedure was used for $[\oplus_0]$. If the differences in positive ion concentrations become too small, the extrapolation becomes unreliable and the procedure is bypassed. Generally integration over 7–12 pulse periods was sufficient to arrive at the steady state.

REFERENCES

1 J. E. Lovelock, *Anal. Chem.*, 33 (1961) 162.
2 W. E. Wentworth, E. Chen and J. E. Lovelock, *J. Phys. Chem.*, 70 (1966) 445.
3 W. E. Wentworth and R. S. Becker, *J. Amer. Chem. Soc.*, 84 (1961) 4263.
4 W. E. Wentworth and J. C. Steelhammer, in E. J. Hart (Editor), *Radiation Chemistry*, American Chemical Society Publications, Washington, D.C., 1968, Ch. 4.
5 D. C. Fenimore, A. Zlatkis and W. E. Wentworth, *Anal. Chem.*, 40 (1968) 1594.
6 R. J. Maggs, P. L. Joynes, A. J. Davies and J. E. Lovelock, *Anal. Chem.*, 43 (1971) 1966.
7 P. L. Patterson, J. Felton, E. Freitas and R. Howe, *1976 Pittsburgh Conference on Applied Spectroscopy, Cleveland, Ohio, March 1976.*
8 E. P. Grimsrud, S. H. Kim, and P. L. Gobby, *Anal. Chem.*, 51 (1979) 223.
9 E. P. Pellizzari, *J. Chromatogr.*, 98 (1974) 323.
10 A. Zlatkis and D. C. Fenimore, *Rev. Anal. Chem.*, 2 (4) (1975) 317.
11 F. W. Karasek and L. R. Field, *Res./Develop*, March 1977.
12 W. E. Wentworth, in I. I. Damsky and J. A. Perry (Editors), *Recent Advances in Gas Chromatography*, Marcel Dekker, New York, 1971, Ch. 5.
13 H. J. van de Wiel and H. Tommassen, *J. Chromatogr.*, 71 (1972) 1.
14 W. E. Wentworth, L. W. Kao and R. S. Becker, *J. Phys. Chem.*, 79 (1975) 1161.
15 C. C. Han, *Master's Thesis*, University of Houston, Houston, Texas, 1969.